International Journal of Technology 13(2) 410-421 (2022)
Received December 2020 / Revised February 2021 / Accepted October 2021

International Journal of Technology

http://ijtech.eng.ui.ac.id

Product Diffusion-Controlled Leaching of Nickel Laterite using Low Concentration Citric Acid Leachant at Atmospheric Condition

Kevin Cleary Wanta[1,3], Widi Astuti[2], Himawan Tri Bayu Murti Petrus[3], Indra Perdana[3*]

[1]*Department of Chemical Engineering, Faculty of Industrial Technology, Parahyangan Catholic University, Jl. Ciumbuleuit 94, Bandung, 40141, Indonesia*
[2]*Research Unit for Mineral Technology, National Research and Innovation Agency (BRIN), Jl. Ir. Sutami Km. 15, Tanjung Bintang, 35361, Indonesia*
[3]*Department of Chemical Engineering, Faculty of Engineering, Universitas Gadjah Mada, Jl. Grafika 2, Bulaksumur, Yogyakarta, 55281, Indonesia*

Abstract. This work studies the leaching kinetics of nickel laterite in a citric acid solution. A new kinetics model that considers a reversible chemical reaction and internal diffusion of a product is proposed. The experiment was conducted at various temperatures (303, 333, and 358 K) and particle sizes (< 70 to 250 μm). Whereas acid concentration, pulp density, and leaching time were constant at 0.1 M, 20% w/v, and 120 min, respectively. The experimental results showed that the leaching process was dependent on temperature and particle size. In the case of Ni, Al, and Fe leachings, the formation of complex molecules might lead to a steric hindrance of product diffusion; however, this was not observable for Mg. The proposed model was found to be much better than the conventional shrinking core models (SCM). Using the proposed model, the activation energy for nickel was found to be 121.38 ± 0.0324 kJ/mol, 78.98 ± 0.4157 kJ/mol, 1,022.62 ± 9.6507 J/mol for forward reaction, backward reaction, and diffusion, respectively.

Keywords: Citric acid; Diffusion model; Leaching kinetics; Nickel laterite; Shrinking core model

1. Introduction

In extractive metallurgy, atmospheric pressure acid leaching (APAL) and bioleaching have been highlighted as options for recovering valuable metals, such as base metals and rare earth elements (Mirwan et al., 2017; Basuki et al., 2020; Trisnawati et al., 2020). These methods have been established and are ready for application on an industrial scale, especially if an intermediate product is preferable for further downstream applications (Rao et al., 2012; Ash et al., 2020). An in-depth study of leaching kinetics is essential to design process equipment for a better industrial-scale application.

Most studies have shown that leaching or bioleaching process kinetics can be approached using the shrinking core model (SCM) (Ayanda et al., 2011; Abilash et al., 2013; Dong et al., 2017; Wang et al., 2017). The SCM is a kinetics model that explains the mechanism of heterogeneous processes, especially for solid-gas reactions (Amiri et al., 2014). The development of this model was mainly based on a single step that controls the

*Corresponding author's email: iperdana@ugm.ac.id, Tel.: +62-22-2508124, Fax: +62-24-555320
doi: 10.14716/ijtech.v13i2.4641

process (Wanta et al., 2016). As a heterogeneous process, the leaching process might consist of a sequence of simultaneous steps. A different assumption might result in a different model, which generates the question of whether the model could explain the actual physical phenomenon. The most common models are derived on the assumption that the kinetics are controlled by the reaction and/or diffusion of the reactant entity (Su et al., 2010; Ayanda et al., 2011; Gharabaghi et al., 2012; Astuti et al., 2016; Mashifana et al., 2019); meanwhile, the limitation of the product entity is rarely explained. Some studies on the leaching process have used inorganic and organic leachates and shown inconsistent results, proving that SCMs would be insufficient to describe the corresponding physical phenomena (Mirwan et al., 2017; Setiawan et al., 2019; Wanta et al., 2020).

The kinetics model of the leaching process has become of interest, as the resulting information can be used for further process development and scale-up purposes. In a leaching process that involves organic acid leachates, there are two unique and different conditions: (1) the formation of metal-organic complex compounds (ligand) (Zelenin, 2007; Jean–Soro et al., 2012; Guilpain et al., 2018), which have a larger molecule size than that of inorganic acid leachates, and (2) reversible reactions associated with acid dissociation and product formation (see Equations 1 and 4) (Zelenin, 2007; Simate et al., 2010; Behera et al., 2011; Horeh et al., 2016). These two conditions can cause the failure of the existing SCM to explain the kinetics of the leaching process, which involves organic acid leachates. This study focuses on developing an alternative and novel mathematical model to describe the kinetics of the leaching process in which organic acid (citric acid solution) is used as a leachate. This model involves the steps that most probably control the leaching process with organic acid leachates: 1) product molecule internal diffusion and 2) reversible chemical reactions. This model is called the product diffusion-controlled model.

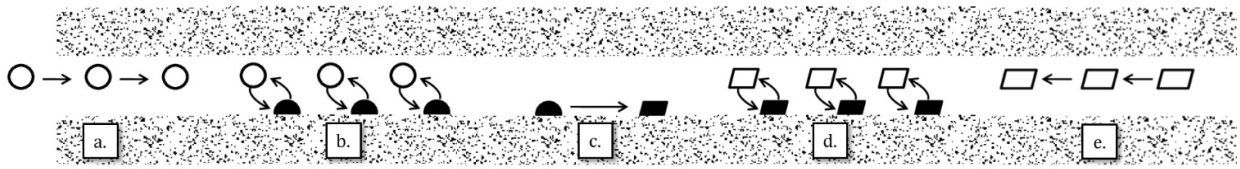

Figure 1 Illustration of the leaching mechanism controlled by the chemical reaction and diffusion of product molecules

The product diffusion-controlled model is arranged according to the mechanism of the leaching process using organic acid (citric acid in this work), as illustrated in Figure 1. Reactant molecules (white spheres in Figure 1a) diffuse through particle pores from the main liquid body. Since the pore size is much larger compared to the reactant molecule diameter, molecular diffusion-type transport is assumed to prevail in the pores. Reactant molecules are then adsorbed into the interior surface to form the adsorbed species (black spheres in Figure 1b), which are always assumed to be in an equilibrium phase. Chemical reactions occur on the solid surface (Figure 1c), as shown in Equations 1–4 (Simate et al., 2010; Behera et al., 2011; Prihutami et al., 2021):

Citric acid dissociation: $C_6H_8O_7 \leftrightarrow (C_6H_5O_7)^{3-} + 3H^+$ (1)

Proton attack: $NiO + 2H^+ \rightarrow Ni^{2+} + H_2O$ (2)

$MCO_3 + 2H^+ \rightarrow M^{2+} + H_2O + CO_2$ (3)

Complexation/chelation: $2(C_6H_5O_7)^{3-} + 3Ni^{2+} \leftrightarrow Ni_3(C_6H_5O_7)_2$ (4)
Nickel citrate complex

Element M in Equation 3 consists of other metal elements, such as Fe, Mg, Al, and so on.

In the case of complex compounds formed as products (black parallelograms in Figure 1c), the adsorbed product molecules will desorb to produce liquid-like free molecules in the pore system (Figure 1d). The concentration of the free molecules is assumed to always be in equilibrium with that of the adsorbed molecules. The equilibrium can be expressed as follows Equations 5:

$$x_p = H.\, C_p \tag{5}$$

where H is a constant, x_p is the concentration of the adsorbed product molecules (ppm), and C_p is the concentration of the free product molecules (ppm). The last step is the movement of product molecules (white parallelograms in Figure 1e) through the pores to the main liquid body. The movement is assumed to be due mainly to molecular diffusion.

In the present work, the proposed model was verified for the leaching of nickel laterite in a low concentration of citric acid. The leaching product of interest is a nickel compound. The development of the material balance for the leached nickel compound inside the solid particle results in Equations 6–8:

$$\frac{\partial C_p}{\partial t} = \frac{De}{\varepsilon}.\left(\frac{\partial^2 C_p}{\partial r^2} + \frac{2}{r}\frac{\partial C_p}{\partial r} + \frac{k_{r,1}}{D_e}x_m - \frac{k_{r,2}}{D_e}x_p\right) \tag{6}$$

$$\frac{dx_m}{dt} = -k_{r,1}x_m + k_{r,2}x_p \tag{7}$$

$$\frac{dC_{p,l}}{dt} = \frac{N_b}{V}4\pi {R_p}^2\left(-D_e\frac{dC_p}{dr}\Big|_{r=R_p}\right) \tag{8}$$

where C_p is the concentration of a liquid-like nickel citrate in the pore channel, D_e is effective diffusivity, ε is porosity, x_m is the concentration of the nickel in a solid phase, $k_{r,1}$ is the reaction rate constant of the product side, $k_{r,2}$ is the reaction rate constant of the reactant side, N_b is the amount of the particle, V is the volume of the solution, R_p is the particle radius, and $C_{p,l}$ is the concentration of the nickel citrate in the liquid body. The equation is numerically solved with the initial and boundary conditions, as shown in the following Equations 9–11:

Initial condition: $C_p = 0,\ x_m = x_{mo}$ (9)

Boundary conditions at the center of particle: $\frac{dC_p}{dr} = 0$ (10)

Boundary conditions at the outer surface of particle: $\frac{dC_p}{dt} = \frac{N_b}{V}4\pi {R_p}^2\left(-D_e\frac{dC_p}{dr}\Big|_{r=R_p}\right)$ (11)

where x_{mo} is the initial concentration of nickel in the solid phase. The low concentration of the citric acid solution used in this work allows the proposed model to be used for further application in the bioleaching process. The proposed model is expected to be more accurate for determining the kinetics parameters needed for further designing the scaled-up extractor.

2. Methods

Nickel laterite was collected from a mining site in Pomalaa, South–East Sulawesi Province, Indonesia. The sample was identified using X-ray fluorescence (S2 Ranger, Bruker) and X-ray diffraction (Ultima IV, Rigaku) with Cu–Kα radiation between 5° and 70° 2θ. The results of the sample analysis are presented in Table 1 and Figure 2. The leaching process was carried out in a three-neck flask container equipped with a static mixer, thermometer, reflux condenser, and the container was put in a heating mantle. A total of 300 ml of 0.1 M citric acid solution was put into the container and mixed with 60 g nickel

laterite sample (20% w/v pulp density). The inclusion of nickel laterite was recorded as t = 0, and the leaching process was initiated.

The leaching process was performed for 2 h at 303, 333, and 358 K. In this work, the particle size was varied in the range of < 70 to 250 μm. For 2 h, samples were taken periodically at 1, 2, 5, 10, 15, 30, 60, and 120 min, followed by a solid-liquid separation using a centrifuge at 1,000 rpm for 10 min. The filtrate (liquid phase) was diluted and analyzed using inductively coupled plasma–optical emission spectroscopy (Optima 8300, Perkin Elmer). In contrast, the solid particles (raw and residue) were analyzed using Quantachrome Instruments version 11.03 to identify the pore diameter. Based on the elemental analysis results, the recovery of each element was determined. In this work, experimental data for nickel recovery were used to verify the acceptability of the proposed kinetics model, which minimizes the sum of errors between experimental data and simulation results. Equations 6–8 were solved simultaneously, along with the respective initial and boundary conditions. The associated kinetics parameters in the model were determined to fit the experimental data. The research methodology mentioned above is illustrated in Figure 3.

Table 1 Chemical compositions of Pomalaa nickel laterite samples

Element	Composition (wt%)
Fe	26.04
Si	15.46
Mg	9.78
Ni	2.73
Al	2.54
Cr	1.01
Mn	0.51
Co	0.07

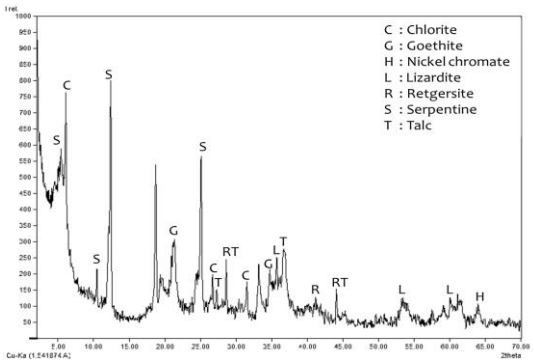

Figure 2 XRD pattern of nickel laterite samples

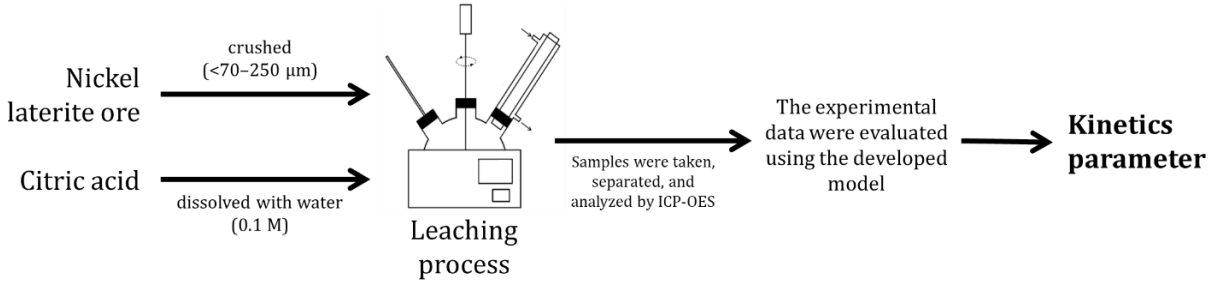

Figure 3 Research methodology scheme

3. Results and Discussion

3.1. Effect of Temperature on Nickel Laterite Leaching Process

Temperature is a critical factor in the leaching process because it determines the rate of the leaching process. Figure 4 shows that the recovery of Ni, Al, Fe, and Mg increased significantly when leaching was conducted at 358 K compared with the others at 303 and 333 K. The particle size used to study this parameter was 125–150 μm.

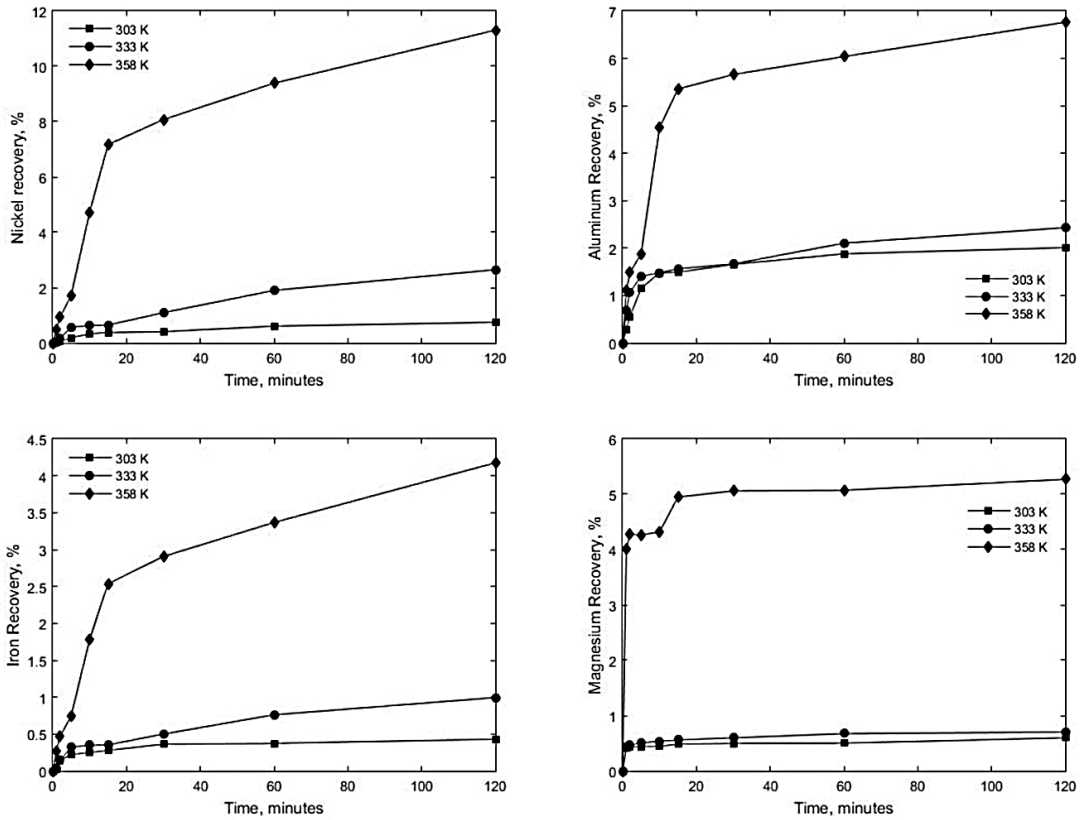

Figure 4 The effect of temperature on nickel laterite processing

A steeper increase in the recovery at 358 K indicates that the leaching process of nickel is strongly activated by temperature. Increasing the temperature leads to faster molecule mobility and a higher possibility of collisions and reactions between molecules. This indicates that a temperature rise affects kinetic energy, both in the reaction and diffusion steps. As described in Equations 1-3, a temperature rise can accelerate the decomposition of the acid to produce protons, which further attack the metals in the solid particles.

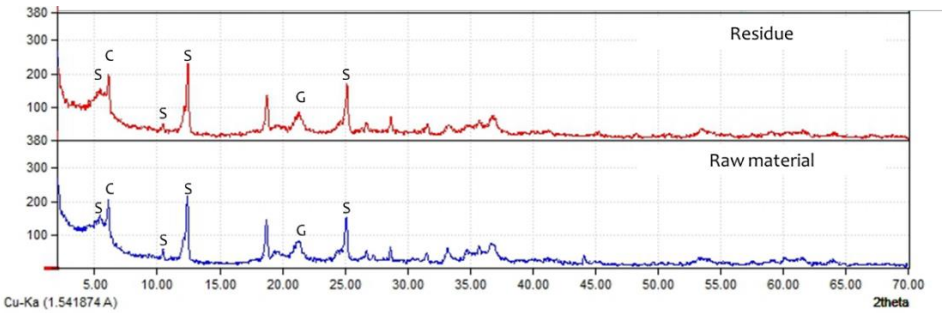

Figure 5 Comparison of XRD patterns between initial and residual samples

The residue from the leaching process was analyzed for possible mineral structure changes, and the results were compared with the initial sample. As shown in Figure 5, the

structure was unaltered, despite an observed slight decrease in the peak intensity. The low concentration of acid used in leaching can preserve the mineral structure. However, as seen in Figure 4, this also leads to a relatively low recovery of metals in a short leaching period.

3.2. Effect of Particle Size on the Nickel Laterite Leaching Process

One of the essential parameters for studying the mechanism of the leaching process is the particle size of the samples. The particle size was varied at <75, 125–150, and 210–250 μm. The metal concentration was assumed to be well distributed in the samples. The experimental results are shown in Figure 6. The figure shows the profile of the concentrations of Ni, Al, Fe, and Mg during a period of leaching. In general, the concentration of elements in the solution increased over time. The increase was rapid in the early stage of leaching and slowed further down in the remaining period. In the case of Ni, Al, and Fe, particle size significantly affected the leaching process. The leaching rate was faster for smaller particles. This might indicate that the diffusion of components in the particles plays an important role. For large particles, the diffusion path was more extended, leading to a slower transport of components. However, for fine particles (< 75 μm), the leaching rate seemed to improve insignificantly because the diffusion resistance inside the particle might be comparable with that of components transported from the solution to the external surface. At this point, the rate of leaching could be further accelerated by increasing the turbulence level of the solution.

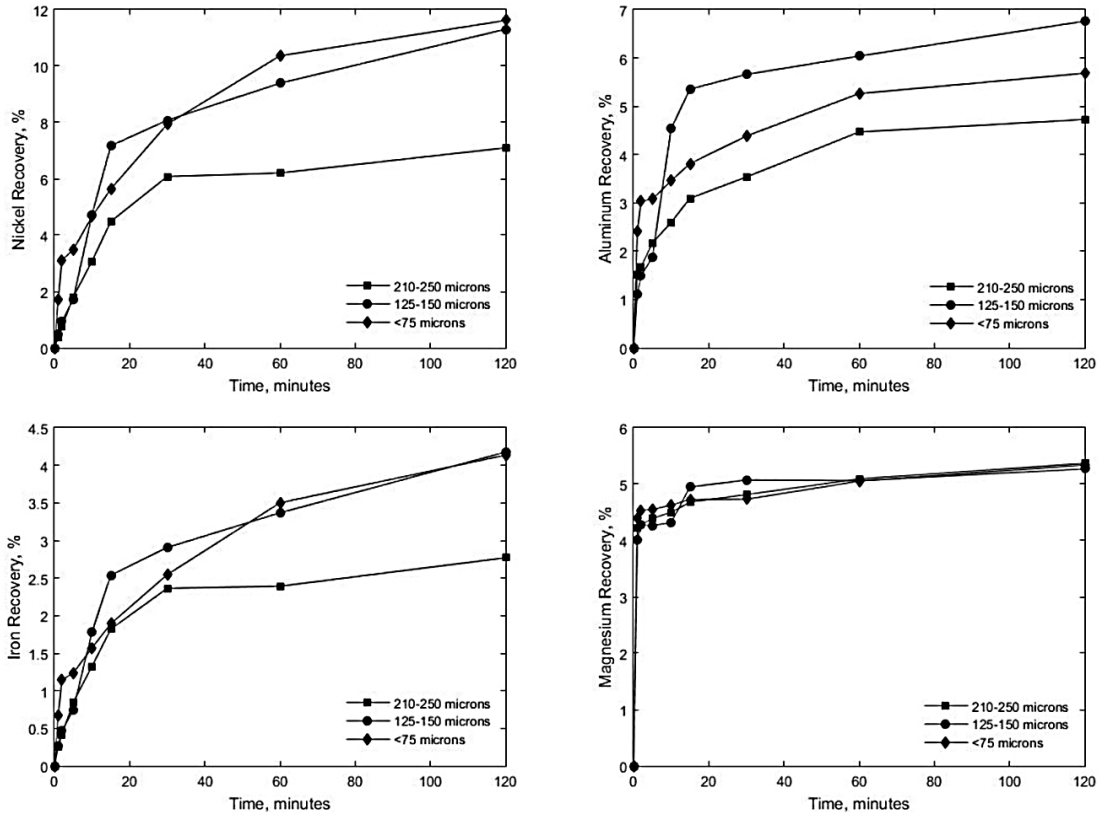

Figure 6 The effect of particle size on the nickel laterite processing

Interestingly, particle size reduction did not always lead to an increased leaching rate for all components. As seen in Figure 6, in the case of magnesium, the recovery was almost unaffected by the particle size. This indicates that the transport of Mg compounds leached from the particle is much easier than the transport of Ni, Al, and Fe compounds. This also

suggests that, in comparison to Ni, Al, and Fe, the leaching of Mg might follow different transport mechanisms.

The transport of components through a porous particle is strongly dependent on the size of the pores and the moving components. This work found that, during the leaching process, the pore diameter of the residue particles enlarged from 25 Å to 43 Å. The associated chemical reactions (Equations 1 to 3) cause the breaking of the intermolecular bonds, producing metal ions that can dissolve in the solution. The leaching of metals from the particles also causes the pore area to become slightly wider than before. However, the change in pore size is also accompanied by the formation of large product molecules that eventually affect the entire leaching kinetics.

In the case of leaching in a citric acid solution, the leached metals could form a large citric acid-associated molecule of chelate. Suppose it is assumed that all molecules are spherical. In that case, the diameters of nickel citrate, aluminum citrate, and iron citrate molecules are estimated at 9.46 Å, 6.7 Å, and 6.7 Å, respectively. In comparison, the diameter of a citric acid molecule (reactant) is estimated at 6.48 Å (National Library of Medicine, 2020). These data show that the size of the chelate molecule is larger than the reactant (citric acid) molecules. The difference in size and the number of moving components will also affect the leaching mechanism.

Leaching is a series of processes of reactant (leachate) transport from the solution bulk to the pores of particles, the reaction of components on the internal particles' surfaces, and product transport from the pores to the bulk. Therefore, the rate of the entire consecutive process is determined by the slowest step. In the case of leaching Ni, Al, and Fe in the citric acid solution, the products seem to form large chelate molecules and diffuse simultaneously in the same path. Although the pore size increases, diffusion through the pores might determine the leaching process because the size of the product molecules is larger. In contrast, as shown in Figure 6, product-controlled transport did not occur in magnesium recovery. The formation of magnesium citrate chelate is unlikely to occur in the particle's pores. This is because the formation of magnesium citrate is slower than the formation of the other associated citric acid molecules with Ni, Al, and Fe. Instead, the leached Mg^{2+} are likely to present and diffuse through the pores into the main liquid body. The size of Mg^{2+} is relatively much smaller, to the extent that the transport does not determine the whole leaching process. Instead, the leaching process is mainly controlled by the reaction rate between citric acid and unreacted components.

3.3. Kinetic Study of the Leaching Process of Nickel Laterite

The mathematical model of the leaching process comprising the reaction and product transport steps that were developed in the Introduction (Equations 6–11) was used to evaluate the leaching of Ni, especially for the leaching process at various temperatures (i.e., 303, 333, and 358 K). As shown in Figure 7, the proposed model can perfectly fit the experimental data. In the case of Ni leaching, the reaction and diffusion of the associated Ni product are temperature activated. This is also an indication that pore channel size strictly limits the diffusion of product molecules through the pores. The molecules might not move freely through the pores, but they preferably need to scrawl on the surface.

The transport model proposed in the present work was compared with two SCMs: (1) conventional diffusion-controlled SCM and (2) chemical and diffusion-controlled (mixed–controlled) SCM. The first SCM model can be represented by the following equation 12 (Ayanda et al., 2011; Agacayak et al., 2016; Rezki et al., 2021):

$$1 - 3(1 - x)^{0.67} + 2(1-x) = k_d.t \quad (12)$$

where x is the reacted fraction, kd is the leaching rate constant, and t is the elapsed time. Equation 12 has been stated as the most appropriate model by several previous researchers (Sahu et al., 2011; Thubakgale et al., 2012; Astuti et al., 2016). The reason is that leaching metals using leachate solution is a diffusion-controlled process, as it involves large molecules. The rate of the leaching process is often suppressed due to prolonged component transport in the interior of particle pores.

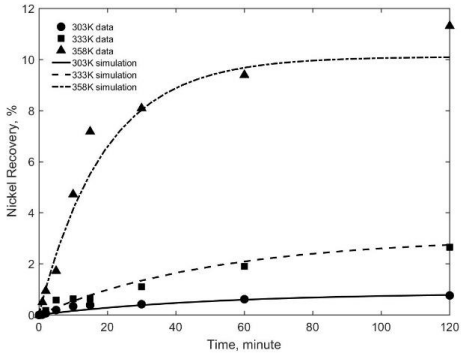

Figure 7 Simulation of a chemical reaction and product diffusion-controlled model for various temperatures

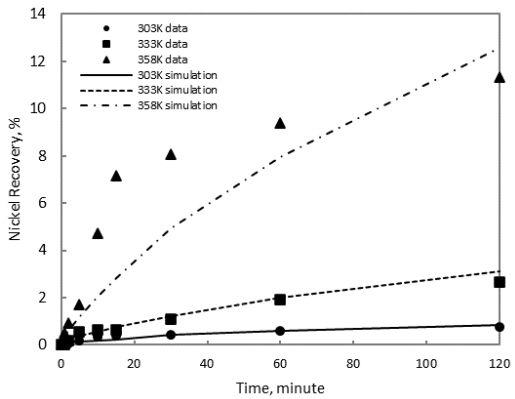

Figure 8 Simulation of mixed-controlled SCM for various temperature

In our other studies (Wanta et al., 2020), the simulation process using Equation 12 and the same experimental data show that the SCM is insufficient to approach the experimental data of the leaching process for nickel laterite Pomalaa using citric acid as the leachate. The commonly used SCM is based on the assumption that the diffusion of reactant molecules determines the process. However, this model might be inappropriate if the product molecules are much larger than the reactants. Furthermore, we also showed that the simulation, which was based on a reactant diffusion-controlled SCM, could not fit the experimental data when the particle size varied in the range of 60–200 meshes (Wanta et al., 2016).

The mixed-controlled model can be represented by the following equation 13 (Ismail et al., 2016):

$$[1 - (1 - x)^{0.33}] + B\,[1 - 0.67X - (1 - x)^{0.67}] = K.t \quad (13)$$

where $B = k_c/k_d$, k_c, and k_d are the chemical reaction and diffusion rate constants from a simple SCM, respectively, and K is the overall leaching rate constant. The model was determined by the consecutive diffusion of the reactant through the ash layer and first-order reaction. The simulation results are presented in Figure 8, which shows that the model is still insufficient for approaching the experimental data, especially at high

temperatures. Quantitatively, a simulation using SCMs resulted in a large percentage of error, namely 141.86% for a diffusion-controlled SCM (Wanta et al., 2020) and 81.33% for a mixed-controlled SCM. This value is significantly greater than the error from the proposed model, which was 23.12%. This strongly suggests that the leaching process in this study is preferably under the simultaneous influence of chemical reactions and internal diffusion of the product molecules.

As proposed in the present work, a mathematical model that considers the diffusion of product molecules is relatively new in hydrometallurgy processes. It has been previously noted that most kinetics studies have shown that the reactant diffusion-controlled SCM was sufficient to model the process. However, the conclusion from those works might be misleading in the case of the leaching process, which resulted in products consisting of large molecules. Results from the present study suggest that, to model a leaching process of metals, it is necessary to consider the nature of the reaction and transport of the involved components. As proposed in the present work and supported by the experimental data, the model for leaching nickel laterite in citric acid leachate should consider the nature of product molecules. If the product is in the form of large molecules, such as ligands, whose size is relatively larger than the reactants, the model should include the reaction and, more importantly, the diffusion of product molecules in the pores.

Based on the model proposed in the present work, some parameters in this model were evaluated. The activation energy (Ea) value was calculated using Equations 14–16 (Callister and Rethwisch, 2015; Astuti et al., 2016):

$$k_{r,1} = k_{ro,1} \cdot \exp\left[-\frac{Ea_{,kr1}}{R}\left(\frac{1}{T}-\frac{1}{T_0}\right)\right] \quad (14)$$

$$k_{r,2} = k_{ro,2} \cdot \exp\left[-\frac{Ea_{,kr2}}{R}\left(\frac{1}{T}-\frac{1}{T_0}\right)\right] \quad (15)$$

$$D_e = D_{eo} \cdot \exp\left[-\frac{Ea_{,De}}{R}\left(\frac{1}{T}-\frac{1}{T_0}\right)\right] \quad (16)$$

where $k_{ro,1}$ is the reaction rate constant to the product side at temperature T_o, $k_{ro,2}$ is the reaction rate constant to the reactant side at T_o, D_{eo} is the effective diffusivity constant at T_o, and R is the gas constant. In the equations, T_o was chosen to be 331.33 K, which is the average operating temperature. The calculation results showed that the values of six constants were as follows:

Table 2 The value of parameter constant in chemical reaction and product diffusion-controlled model

Parameter	Value
$k_{ro,1}$ (1/min)	0.0023 ± 0.000005
$k_{ro,2}$ (1/min)	0.0010 ± 0.000007
D_{eo} (cm^2/min)	0.0054 ± 0.000262
$Ea_{,kr1}$ (kJ/mol)	121.38 ± 0.0324
$Ea_{,kr2}$(kJ/mol)	78.98 ± 0.4157
$Ea_{,De}$(kJ/mol)	1,022.62 ± 9.6507

These six parameters complied with the relatively small 95% interval confidences for each parameter. The results indicate that the constants obtained have a high level of confidence. The activation energy values for the chemical reaction steps are much higher than the diffusion steps. This means that the diffusion steps are not influenced by temperature. Table 3 shows that the effective diffusivity constant does not increase

significantly with temperature. In addition, as shown in Table 3, the reaction rate constants increase more significantly as the temperature rises.

Table 3 The value of reaction and diffusion constant at various temperatures

Temperature, K	Reaction rate constant to product side ($k_{r,1}$), /min	Reaction rate constant to reactant side ($k_{r,2}$), /min	Effective diffusivity constant (D_e), cm^2/min
303	0.00022	0.00010	0.00535
333	0.00229	0.00099	0.00539
358	0.01448	0.00742	0.00546

Compared to the activation energy values (forward reaction) obtained from the present study, some values from previous studies have lower values (Ayanda et al., 2011; Girgin et al., 2011; Thubakgale et al., 2012; Agacayak et al., 2016). Therefore, the present study shows that the leaching of Pomalaa nickel laterite in low-concentration citric acid leachate needs more energy to recover the nickel from the ore.

4. Conclusions

This work presented a study to experimentally prove that the diffusion of products determines the rate of the leaching process of nickel laterite. In the case of leaching Ni, Al, and Fe from the mineral, the resulting products consisted of relatively large molecules, whose transport was sterically hindered in the pore channels. Meanwhile, leached Mg was present in ionic forms; hence, its transport through the pores did not determine the leaching process. The proposed mathematical model, considering the steps of reaction and transport of product molecules, was suitable for describing the Ni leaching process phenomenon. The model will be applicable to a similar process that incorporates large product molecules.

Acknowledgements

The authors gratefully acknowledge the Department of Chemical Engineering, Universitas Gadjah Mada, for assistance with the sample analysis. In addition, the authors acknowledge Research Unit for Mineral Technology, National Research and Innovation Agency (BRIN) for providing samples and chemical analysis.

References

Abilash, Mehta, K.D., Pandey, B.D., 2013. Bacterial Leaching Kinetics for Copper Dissolution from a Low-Grade Indian Chalcopyrite Ore. *Metalurgia e Materials (Metallurgy and Materials)*, Volume 66(2), pp. 245–250

Agacayak, T., Zedef, V., Aras, A., 2016. Kinetic Study on Leaching of Nickel from Turkish Lateritic Ore in Nitric Acid Solution. *Journal of Central South University,* Volume 23, pp. 39–43

Amiri, A., Ingram, G.D., Maynard, N.E., Livk, I., Bekker, A.V., 2014. An Unreacted Shrinking Core Model for Calcination and Similar Solid–to–Gas Reactions. *Chemical Engineering Communications*, Volume 202(9), pp. 1161–1175

Ash, B., Nalajala, V.S., Popuri, A.K., Subbaiah, T., Minakshi, M., 2020. Perspectives on Nickel Hydroxide Electrodes Suitable for Rechargeable Batteries: Electrolytic vs. Chemical Synthesis Route. *Nanomaterials,* Volume 10(9), pp. 1–22

Astuti, W., Hirajima, T., Sasaki, K., Okibe, N., 2016. Comparison of Atmospheric Citric Acid Leaching Kinetics of Nickel from Different Indonesian Saprolitics Ores. *Hydrometallurgy*, Volume 161, pp. 138–151

Ayanda, O.S., Adekola, F.A., Baba, A.A., Fatoki, O.S., Ximba, B.J., 2011. Comparative Study of the Kinetics of Dissolution of Laterite in Some Acidic Media. *Journal of Minerals & Materials Characterization & Engineering*, Volume 10(15), pp. 1457–1472

Basuki, K.T., Rohmaniyyah, A., Pusparini, W.R., Saputra, A., 2020. Extraction Development for the Separation of Gadolinium from Yttrium and Dysprosium Concentrate in Nitric Acid Using Cyanex 572. *International Journal of Technology*, Volume 11(3), pp. 450–460

Behera, S.K., Panda, P.P., Singh, S., Pradhan, N., Sukla, L.B., Mishra, B.K., 2011. Study on Reaction Mechanism of Bioleaching of Nickel and Cobalt from Lateritic Chromite Overburdens. *International Biodeterioration & Biodegradation*, Volume 65, pp. 1035–1042

Callister, W.D., Rethwisch, D.G., 2015. *Materials Science and Engineering*. 9th Edition. USA: John Wiley & Sons

Dong, Y.-b., Li, H., Lin, H., Zhang, Y., 2017. Dissolution Characteristics of Sericite in Chalcopyrite Bioleaching and Its Effect on Copper Extraction. *International Journal of Minerals, Metallurgy, and Materials*, Volume 24(4), pp. 369–376

Gharabaghi, M., Irannajad, M., Azadmehr, A.R., 2012. Leaching Behavior of Cadmium from Hazardous Waste. *Separation and Purification Technology*, Volume 86, pp. 9–18

Girgin, İ., Obut, A., Üçyildiz, A., 2011. Dissolution Behaviour of a Turkish Lateritic Nickel Ore. *Minerals Engineering*, Volume 24(7), pp. 603–609

Guilpain M., Laubie, B., Zhang, X., Lorel J.L., Simonnot, M.-O., 2018. Speciation of Nickel Extracted from Hyperaccumulator Plants by Water Leaching. *Hydrometallurgy*, Volume 180, pp. 192–200

Horeh, N.B., Mousavi, S.M., Shojaosadati, S.A., 2016. Bioleaching of Valuable Metals from Spent Lithium-Ion Mobile Phone Batteries using *Aspergillus niger*. *Journal of Power Sources*, Volume 320, pp. 257–266

Ismail, S., Hussin, H., Hashi, S.F.S., Abdullah, N.S., 2016. Leaching and Kinetic Modeling of Malaysian Low-Grade Manganese Ore in Sulfuric Acids. *Advanced Materials Research*, Volume 1133, pp. 629–633

Jean–Soro, L., Bordas. F., Bollinger, J.-C., 2012. Column Leaching of Chromium and Nickel from a Contaminated Soil Using EDTA and Citric Acid. *Environmental Pollution*, Volume 164, pp. 175–181

Mashifana, T., Ntuli, F., Okonta, F., 2019. Leaching Kinetics on the Removal of Phosphorus from Waste Phosphogypsum by Application of Shrinking Core Model. *South African Journal of Chemical Engineering*, Volume 27, pp. 1–6

Mirwan, A., Susianto, Altway, A., Handogo, R., 2017. A Modified Shrinking Core Model for Leaching of Aluminum from Sludge Solid Waste of Drinking Water Treatment. *International Journal of Technology*, Volume 8(1), pp. 19–26

National Library of Medicine—National Center for Biotechnology Information, 2020. Nickel Citrate, Aluminium Citrate, Iron Citrate, Citric Acid. Available Online at https://pubchem.ncbi.nlm.nih.gov/, Accessed on May 5, 2020

Prihutami, P., Prasetya, A., Sediawan, W.B., Petrus, H.T.B.M., Anggara, F., 2021. Study on Rare Earth Elements Leaching from Magnetic Coal Fly Ash by Citric Acid. *Journal of Sustainable Metallurgy*, Volume 7, pp. 1241–1253

Rao, S.V., Dong, H.Y., Jeong, S.S., Kim, S.-K., 2012. Purification of Sulphate Leach Liquor of Spent Raneynickel Catalyst Containing Al and Ni by Solvent Extraction with

Organophosphorus–Based Extractants. *The Scientific World Journal*, Volume 2012, pp. 1–5

Rezki, A.S., Sumardi, S., Astuti, W., Bendiyasa, I.M., Petrus, H.T.B.M, 2021. Molybdenum Extraction from Spent Catalyst Using Citric Acid: Characteristic and Kinetics Study. *IOP Conf. Series: Earth and Environmental Science*, Volume 830, pp. 1–10

Sahu, S., Kavuri, N.C., Kundu, M., 2011. Dissolution Kinetics of Nickel Laterite Ore using Different Secondary Metabolic Acids. *Brazilian Journal of Chemical Engineering*, Volume 28(2), pp. 251–258

Setiawan, H., Petrus, H.T.B.M., Perdana, I., 2019. Reaction Kinetics for Lithium and Cobalt Recovery from Spent Lithium-Ion Batteries using Acetic Acid. *International Journal of Minerals, Metallurgy, and Materials*, Volume 26(1), pp. 98–107

Simate, G.S., Ndlovu, S., Walubita, L.F., 2010. The Fungal and Chemolithotrophic Leaching of Nickel Laterites—Challenges and Opportunities. *Hydrometallurgy*, Volume 103, pp. 150–157

Su, H., Liu, H., Wang, F., Lü, X., Wen, Y., 2010. Kinetics of Reductive Leaching of Low–Grade Pyrolusite with Molasses Alcohol Wastewater in H_2SO_4. *Chinese Journal of Chemical Engineering*, Volume 18(5), pp. 730–735

Thubakgale, C.K., Mbaya, R.K.K., Kabongo, K., 2012. Leaching Behaviour of a Low–Grade South African Nickel Laterite. *International Journal of Materials and Metallurgical Engineering*, Volume 6(8), pp. 761–765

Trisnawati, I., Prameswara, G., Mulyono, P., Prasetya, A., Petrus, H.T.B.M., 2020. Sulfuric Acid Leaching of Heavy Rare Earth Elements (HREEs) from Indonesian Zircon Tailing. *International Journal of Technology*, Volume 11(4), pp. 804–816

Wang, Y., Jin, S., Lv, Y., Zhang, Y., Su, H., 2017. Hydrometallurgical Process and Kinetics of Leaching Manganese from Semi–Oxidized Manganese Ores with Sucrose. *Minerals*, Volume 7(27), pp. 1–13

Wanta, K.C., Astuti, W., Perdana, I., Petrus, H.T.B.M., 2020. Kinetic Study in Atmospheric Pressure Organic Acid Leaching: Shrinking Core Model. *Minerals*, Volume 10(7) pp. 1–10

Wanta, K.C., Perdana, I., Petrus, H.T.B.M., 2016. Evaluation of Shrinking Core Model in Leaching Process of Pomalaa Nickel Laterite Using Citric Acid as Leachate at Atmospheric Conditions. *In:* IOP Conference Series: Materials Science and Engineering, Volume 162, pp. 1–5

Zelenin, O.Y., 2007. Interaction of the Ni^{2+} Ion with Citric Acid in an Aqueous Solution. *Russian Journal of Coordination Chemistry*, Volume 33(5), pp. 346–350